Materials Science & Engineering A 781 (2020) 139246

Contents lists available at ScienceDirect

Materials Science & Engineering A

journal homepage: www.elsevier.com/locate/msea

# Indentation creep vs. indentation relaxation: A matter of strain rate definition?

Paul Baral [a,b,*], Guillaume Kermouche [b], Gaylord Guillonneau [a], Gabrielle Tiphene [a], Jean-Michel Bergheau [c], Warren C. Oliver [d], Jean-Luc Loubet [a]

[a] Univ. Lyon, Ecole Centrale de Lyon, CNRS UMR 5513 LTDS, F-69134, Ecully, France
[b] Mines Saint Etienne, Université de Lyon, CNRS UMR 5307 LGF, Centre SMS, F-42023, Saint Etienne, France
[c] Univ. Lyon, Ecole Nationale d'Ingénieurs de Saint Etienne, CNRS UMR 5513 LTDS, F-42023, Saint Etienne, France
[d] KLA Nanomechanics Inc., Oak Ridge, TN 37830, USA

ARTICLE INFO

*Keywords:*
Nanoindentation
Strain rate sensitivity
Relaxation
Creep
Selenium

ABSTRACT

An extensive study of the different methods able to measure material creep properties in indentation is proposed. A systematic comparison of the fast creep, long-term creep, constant strain rate and long-term relaxation tests is performed on amorphous selenium. Even though measured apparent activation energy and strain rate sensitivities are very similar for all tests, a discrepancy is highlighted between the creep/constant strain rate tests and the relaxation tests. This effect seems to be related to the strain rate definition which should be a function of the strain rate sensitivity $m$. In this paper, it is proposed to use a representative strain rate $\dot{\epsilon}_r$ as proposed by Kermouche et al. (2008). An excellent agreement is found between all the methods, including uniaxial compression when expressing the creep behavior as a function of representative stress and strain rate.

## 1. Introduction

Current developments in high temperature nanoindentation testing allow the measurements of material mechanical properties up to 1000 °C and certainly more in the near-future [1–5]. This opens a new research area dedicated to the characterization of material creep and relaxation properties at a very small scale. Indeed, the increasing developments of engineering surfaces such as layered coatings and tribo-films able to withstand extreme contact conditions bring a particular interest to high temperature nanoindentation.

However, the measurement of intrinsic creep properties using nanoindentation is still at stake. Some pioneering works highlighted the ability of instrumented indentation to measure strain rate sensitivity $m$ and activation energy $Q$ from hardness versus time – or strain rate – measurements [6,7]. All these works aim to relate uniaxial stress and strain rate to indentation measurements such as hardness, stiffness and penetration depth. However, those developments are only approximations based on restrictive assumptions [6,8]. Yet, constant strain rate or indentation creep tests were scrutinized by many authors to eventually conclude that they were reliable [9–14].

Indentation relaxation tests were less explored due to technical difficulties — i.e. thermal drift and displacement control overshoot [15,16]. Therefore, only a few comparisons between indentation creep and indentation relaxation have been published. Nonetheless, indentation relaxation may present some advantages compared to indentation creep when indenting thin films or materials exhibiting size effects. Actually, the plastic – or viscoplastic – volume barely changes during the relaxation – constant contact area – segment whereas it can significantly increase during a creep – constant load – segment. Besides, as the plastic volume increases, more and more material is subjected to primary creep which could lead to erroneous measurements of the stationary creep parameters [15]. As a result, indentation creep is more prone to measurement artifacts arising from the variation of probed volume during the hold segment. Recently, Baral et al. [17] found an original way to overcome most of the indentation relaxation related issues so benchmarking indentation creep against relaxation is possible now. It is worth noting that extraction of creep data from these two kinds of loadings strongly differs. On one hand the computation of strain rate is directly related to hardness – for relaxation – and on the other hand it is related to penetration depth or contact stiffness — for creep. Therefore, the strain rate definition might be under discussion.

In this paper, it is proposed to challenge the ability of indentation creep and indentation relaxation to measure creep properties of a widely investigated model material that exhibits significant creep at room temperature — amorphous selenium. First, the basic theoretical

* Corresponding author at: Univ. Lyon, Ecole Centrale de Lyon, CNRS UMR 5513 LTDS, F-69134, Ecully, France.
*E-mail address:* paul.baral@ec-lyon.fr (P. Baral).

https://doi.org/10.1016/j.msea.2020.139246
Received 21 January 2020; Received in revised form 1 March 2020; Accepted 11 March 2020
Available online 13 March 2020
0921-5093/

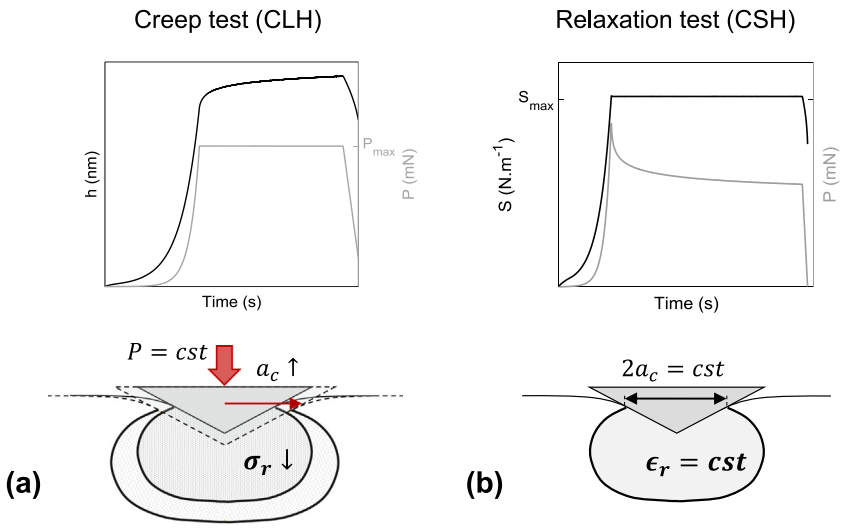


**Fig. 1.** Schematic of indentation (a) creep and (b) relaxation tests. The upper parts represent the load and displacement – or contact stiffness – versus time for both tests. The lower schemata display the stress and strain fields under an axisymmetric tip for creep and relaxation, respectively.

features of constant strain rate, indentation creep and indentation relaxation are presented. Then the experimental methodology is developed. Results are presented in terms of strain rate versus hardness curves. The observed shift between indentation creep and indentation relaxation is discussed, questioning the strain rate definition in indentation creep. In the end, a new strain rate definition is proposed.

## 2. Theoretical framework

### 2.1. Creep tests

The indentation creep test is defined by a constant load hold segment while the displacement $h$ [7] or, more recently, contact stiffness $S$ [18,19] is monitored as shown on the graph in Fig. 1a. During the test, the contact radius $a_c$ continuously grows as the material creeps. The hardness $H$ also referred as mean contact pressure $p_m$ is defined by the load $P$ divided by the projected contact area $A_c$ (Eq. (1)). The latter can be related to a uniaxial representative stress $\sigma_r = \frac{H}{\gamma}$, with $\gamma$ the reduced contact pressure [6,20]. So, during an indentation creep test, the representative stress $\sigma_r$ drops (Fig. 1a).

$$H = \frac{P}{A_c} \tag{1}$$

The indentation strain rate $\dot{\epsilon}^{ind}$ is simply expressed from the movement of the indenter into the material, as:

$$\dot{\epsilon}^{ind} = \frac{\dot{h}}{h} = \frac{\dot{S}}{S} \tag{2}$$

This type of loading implies that the volume of indented material increases with time, which can lead to non trivial estimation of creep properties [15].

### 2.2. Relaxation tests

The indentation relaxation test aims at maintaining a constant contact area $A_c$ between the indenter and the material while monitoring the load. This can be done by keeping the displacement constant [16,21,22], assuming that the contact geometry remains the same and the thermal drift is negligible. Current developments by Baral et al. [17] proposed to control the contact stiffness rather than the displacement to ignore the contact geometry or thermal stability considerations (Fig. 1b). The advantage of this method is that the probed volume barely changes as well as the applied strain which is basically dependent on the indenter geometry — half-included angle $\theta$ for a conical indenter.

Yet, whereas the hardness can be formulated from Eq. (1), the concept of strain rate cannot be described with Eq. (2) since $\dot{h}$ or $\dot{S}$ should be zero. Baral et at. [17] proposed a definition of strain rate during relaxation $\dot{\epsilon}^{rel}$ in analogy with the uniaxial relaxation of a power law creeping solid:

$$\dot{\epsilon}^{rel} = \frac{1}{E'}\frac{d\sigma_r}{dt} \tag{3}$$

With $E'$ the Young modulus and $\sigma_r$ the representative stress. In the following developments, the formulation of representative stress expressed by Kermouche et al. [8] based on the conical indentation of an elastoplastic solid will be used:

$$\sigma_r = \frac{\zeta_3 \cot(\theta) H}{\zeta_1 \cot(\theta) - (1-\zeta_2)\frac{H}{E'}} \tag{4}$$

With geometrical constants $\zeta_1 = 0.66$, $\zeta_2 = 0.216$ and $\zeta_3 = 0.24$, for a cone of half-included angle $\theta = 70.32°$ — i.e. Berkovich indenter. Details on the developments of Eq. (4) can be found elsewhere [8,23].

### 2.3. Strain rate sensitivity

In uniaxial tests the strain rate sensitivity $m$ characterizes the variation of yield stress with the corresponding applied strain rate, which is given by $\sigma = \frac{1}{\alpha}\dot{\epsilon}^m$ for power law creeping solids, with $\alpha$ the consistency. Within indentation experiments, the strain rate sensitivity is often measured through the following approximation:

$$m \approx \frac{d\ln H}{d\ln \dot{\epsilon}} \tag{5}$$

It must be noted that, in the framework of rigid viscoplastic solids, Eq. (5) is no longer an approximation but an exact solution. Regarding elastic-viscoplastic solids, it has been shown that the discrepancy increases when $H/E'$ increases [10,24]. The use of representative stress instead of hardness in Eq. (5) allows to get a better approximation of strain rate sensitivity [25]. In the following developments, the uniaxial definition of strain rate sensitivity, noted $m$, will be used. Even though, the experimental results will be computed as *indentation* strain rate sensitivity (Eq. (5)) for comparison with previous studies.

## 3. Materials and methods

The selenium used in this study is chemical grade 5 nines pure and was purchased in the form of crystallized blocks. The blocks were melted in a beaker on a hot plate and then quenched into copper molds

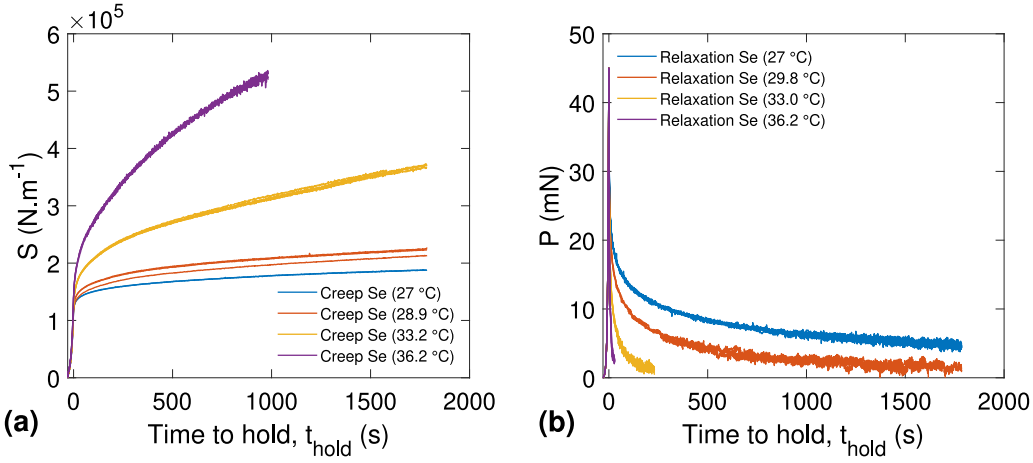


**Fig. 2.** Contact stiffness and load as a function of holding time $t_{hold}$ for CLH-S creep tests (a) and CSH relaxation tests (b) at different temperatures.

in order to get amorphous selenium. The as-cast sample was 31.75 mm in diameter and around 5 mm in thickness with a mirror-like surface. Nanoindentation tests were performed using a KLA Nanomechanics iNano® equipped with a Berkovich diamond tip. The whole apparatus was placed into a thermally-isolated box with a heater. The temperature was monitored with a resolution of 0.01 °C from a thermocouple placed close to the nanoindenter, in the isolated-chamber. A constant power was set to the heater and twelves hours were necessary to reach thermal equilibrium inside the chamber. At each temperature, 4 to 6 tests were performed using constant strain rate (CSR), fast creep, long-term creep and long-term relaxation. Each test was performed at a maximum load of 45 mN.

For constant strain rate as well as long-term creep and relaxation tests, the continuous stiffness measurement (CSM®) module was used. It was developed by Pethica and Oliver [26] to allow the measurement of contact stiffness as a function of indentation depth. It has been assessed by several authors [18,27] that contact area is proportional to the contact stiffness as long as the materials' modulus is not indentation depth-dependent. Therefore, the following relation is used [28]:

$$A_c = \frac{\pi}{4}\left(\frac{S(\omega)}{E_c'^*(\omega)}\right)^2 \tag{6}$$

where $E_c'^*(\omega)$ is the reduced contact modulus [29] calculated at a given frequency $\omega$ from the Oliver and Pharr method [27] and $S(\omega)$ is the contact stiffness at the same frequency.

Stiffness measurements were performed at 100 Hz frequency with a fixed force amplitude equal to 3% of the current applied load in order to get the best calculation from the lock-in amplifier [30].

In the following, the different types of experiments are detailed.

### 3.1. Constant strain rate tests

For the constant strain rate test (CSR), the load is increased as an exponential function of time in order to obtain a constant $\dot{P}/P$. Assuming that hardness does not vary with indentation depth, the following relation can be written, $\dot{\epsilon}^{ind} = \frac{\dot{h}}{h} = \frac{1}{2}\frac{\dot{P}}{P}$ [9]. The CSR tests were performed at 5 indentation strain rates as detailed in Table 1.

### 3.2. Fast creep tests

Fast creep tests were performed with a constant loading rate, where the maximum load (45 mN) is reached in 0.5 s, then the load is maintained constant and the displacement is monitored during 30 s. This procedure allows to get additional information on the fast creep behavior of the material. The continuous stiffness measurement is switched-off, so only load and displacement are used to calculate the mechanical properties [2]. Therefore, the hardness is calculated from this expression:

$$H = \frac{P}{\pi a_c^2} = \frac{P}{\pi(\xi h)^2} \tag{7}$$

With $a_c$ assumed to be a constant function of $h$ determined from preliminary CSR tests performed with the continuous stiffness measurement (CSM®). Hence, we can calculate the equivalent contact radius $a_c = S/(2E_c'^*)$, with $E_c'^*$ the reduced contact modulus [29] and evaluate the ratio $\xi = a_c/h$. This ratio accounts for the pile up or sink in contact geometry around the tip and may change as a function of the temperature and material's strain rate sensitivity [6,31]. In the case of fast creep test, the range of measured strain rates is sufficiently narrow to assess a constant strain rate sensitivity $m$ and therefore a constant ratio $\xi$. The latter has been evaluated at the beginning of the hold segment for both long-term creep and relaxation tests. As it does not vary much with temperature, it is taken to be constant with $\xi = 2.43$.

**Table 1**
Measured indentation strain rates $\dot{\epsilon}_i^{ind} = \dot{h}/h$ at the end of loading during the CSR experiments for all the tested temperatures.

| Temperature | 27 °C | 30 °C | 33 °C | 36 °C |
|---|---|---|---|---|
| $\dot{\epsilon}_1^{ind}$ | $4.95E^{-3}$ $s^{-1}$ | $1.28E^{-2}$ $s^{-1}$ | $1.39E^{-2}$ $s^{-1}$ | $2.35E^{-2}$ $s^{-1}$ |
| $\dot{\epsilon}_2^{ind}$ | $1.31E^{-2}$ $s^{-1}$ | $2.65E^{-2}$ $s^{-1}$ | $3.03E^{-2}$ $s^{-1}$ | $3.42E^{-2}$ $s^{-1}$ |
| $\dot{\epsilon}_3^{ind}$ | $2.64E^{-2}$ $s^{-1}$ | $5.40E^{-2}$ $s^{-1}$ | $5.60E^{-2}$ $s^{-1}$ | $6.21E^{-2}$ $s^{-1}$ |
| $\dot{\epsilon}_4^{ind}$ | $5.22E^{-2}$ $s^{-1}$ | $1.04E^{-1}$ $s^{-1}$ | $1.05E^{-1}$ $s^{-1}$ | $1.16E^{-1}$ $s^{-1}$ |
| $\dot{\epsilon}_5^{ind}$ | $1.10E^{-1}$ $s^{-1}$ | $1.55E^{-1}$ $s^{-1}$ | $1.62E^{-1}$ $s^{-1}$ | $1.70E^{-1}$ $s^{-1}$ |

### 3.3. Long-term creep tests

Long-term creep tests were performed with an exponential loading at constant indentation strain rate of $\dot{\epsilon}^{ind} = 1.06E^{-1}$ $s^{-1}$ followed by a constant load segment of 30 min. For experiments performed at 36 °C, holding time was limited to 17 min because maximum displacement was reached during the creep segment. In this experiment, the contact stiffness $S$ is measured continuously with the CSM® module as shown in Fig. 2a. As a result, the creep behavior is only monitored from the contact stiffness evolution since the latter is less affected by the thermal drift than displacement [18,19]. Indeed, on Fig. 2a four to six tests are displayed for each temperature, highlighting the excellent stability and repeatability of the measurements.

The hardness is calculated by replacing the contact area $A_c$ from Eq. (1) by Eq. (6).

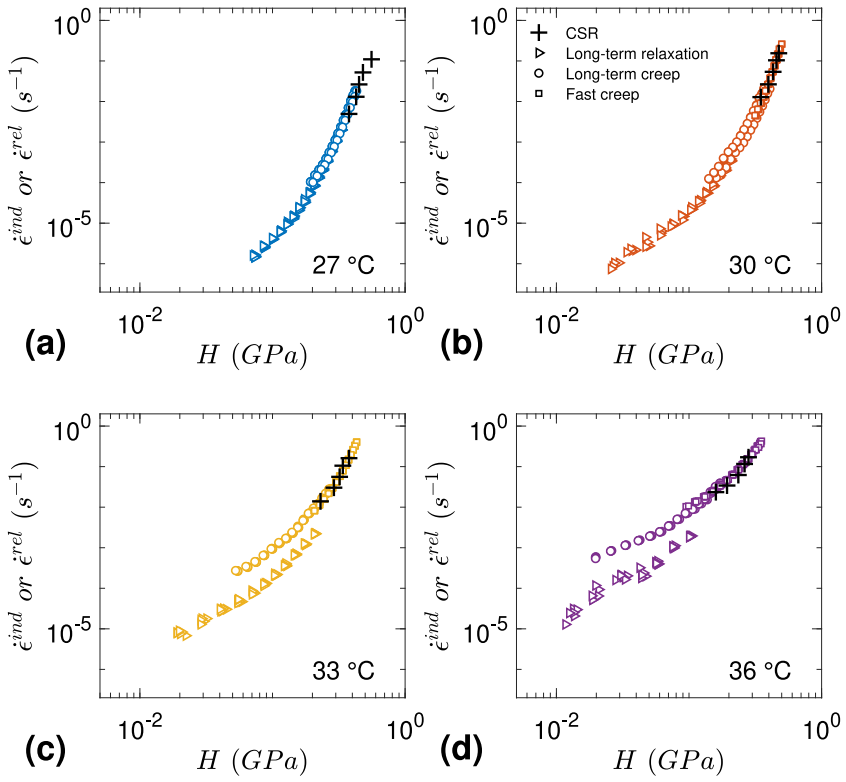


**Fig. 3.** Indentation creep behavior of amorphous selenium measured from CSR (plus symbols), fast creep (square symbols), long-term creep (circle symbols) and relaxation (right pointing triangle symbols) at different temperatures: (a) 27 °C, (b) 30 °C, (c) 33 °C and (d) 36 °C.

### *3.4. Long-term relaxation tests*

Finally, Long-term relaxation tests were achieved with an exponential loading at constant indentation strain rate of $\dot{\epsilon}^{ind} = 1.05E^{-1}$ s$^{-1}$ followed by a constant stiffness segment. The duration of this segment was varied from 30 min for tests performed at 27 °C and 30 °C to 250 s for tests at 33 °C and 70 s for tests at 36 °C. It was done because the load nearly dropped to zero during the relaxation segment as shown in Fig. 2b. Therefore, as the CSM® force amplitude was a percentage of the applied load, this amplitude dropped to zero as well, making the measurement of the stiffness very noisy and by extension difficult to control. Contact stiffness $S$ was maintained constant through a PID loop where only proportional and integral gains were tuned [17]. Here again, measurements are remarkably reproducible — four to six tests are displayed for each temperature (Fig. 2b).

As for the long-term creep test, the hardness is calculated by replacing the contact area $A_c$ from Eq. (1) by Eq. (6).

## 4. Results and discussion

The creep behavior derived from indentation experiments is described by the evolution of indentation strain rate with hardness. Fig. 3 displays those graphs for the four temperatures tested. All the types of tests are compared and four to six curves by test are represented to assess the repeatability of the different methods. All the curves are onto the same master curve for temperature below 30 °C but a shift appears for higher temperatures between the relaxation tests on one side and the creep tests and the constant strain rate tests on the other side: The higher the temperature, the larger the shift. However, the general trends of the measured creep behaviors are in good agreement.

Indentation strain rate sensitivity $m$ has been calculated for fast creep tests, long-term creep tests and long-term relaxation tests by dividing the curves of Fig. 3 in three hardness ranges equally spaced in a log-scale and then by fitting each of the portion with Eq. (5). Strain rate sensitivity for CSR tests has also been computed by fitting the whole of the data for tests at 27 °C and 30 °C and two halves for 33 °C and 36 °C.

Results are plotted as a function of strain rate and temperature in Fig. 4. The results are in quite good agreement but a significant mismatch is observed at high temperature — $T$ °C $>$ 33 °C. The estimated apparent activation energy (see Appendix) is quite similar for both cases, which points out that this difference is not directly related to temperature. It is worth noting that amorphous selenium is known to exhibit a significant variation of strain rate sensitivity near its glass transition. This is also observed here, with $m$ close to 1 above 35 °C [31]. Besides, amorphous selenium is not expected to present several deformation mechanisms that could be triggered by different loadings — i.e. constant load or constant contact stiffness. Hence, the observed mismatch/shift between indentation creep and indentation relaxation results should not arise from material's intrinsic behavior. The role of strain rate sensitivity on this mismatch has thus to be explored.

To investigate this point in detail, it is necessary to remind the notions of representative stress, strain and strain rate in indentation. This concept, first introduced by Tabor [32] seventy years ago, states that a representative stress and a representative strain, that corresponds to each other on the uniaxial stress–strain curve, can be related to hardness, Young modulus and tip angle in the framework of elastoplastic solids' sharp indentation [33].

Based on this, extensive studies have yielded various analytical expressions of these representative parameters [8,34–36].

In the framework of viscous solids, the same kind of approach has been derived to define a representative strain rate [7,8,36]. Still, it has been significantly less explored.

Let us apply this concept to power law creeping solids, for which the uniaxial relation between some representative stress and strain rate is given by:

$$\dot{\epsilon_r} = \alpha \sigma_r^{(1/m)} \tag{8}$$

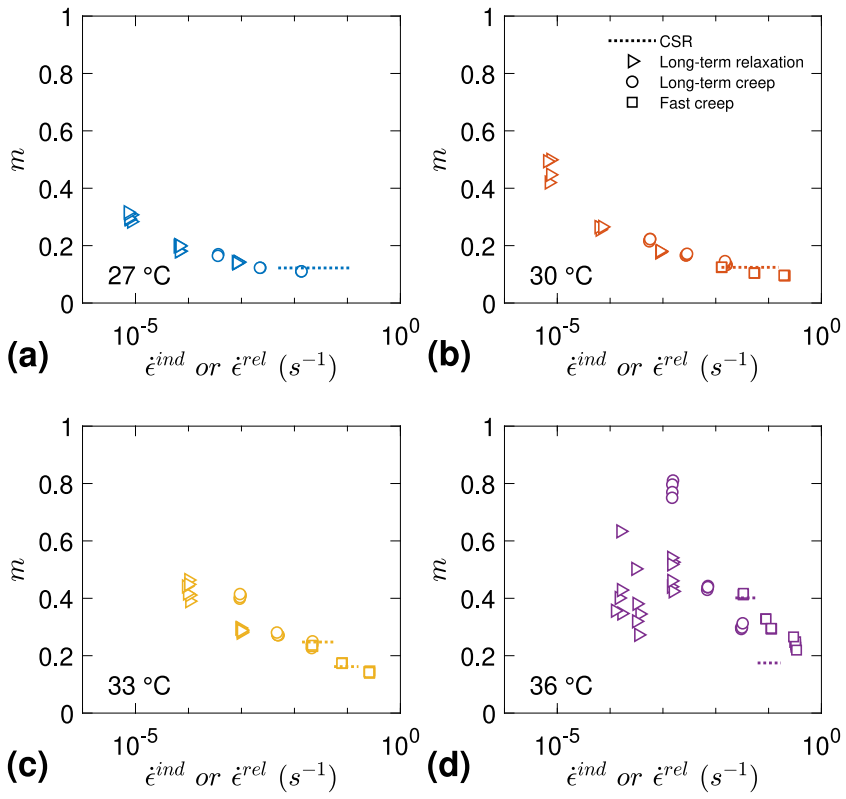


**Fig. 4.** Indentation strain rate sensitivity $m$ as a function of indentation strain rate either calculated with $\dot{\epsilon}^{ind}$ (Eq. (2)) for creep and CSR tests or $\dot{\epsilon}^{rel}$ (Eq. (3)) for relaxation tests: (a) 27 °C, (b) 30 °C, (c) 33 °C and (d) 36 °C.

where consistency $\alpha$ and strain rate sensitivity $m$ are material constants. It has been demonstrated by number of authors [2,9,15] that nanoindentation creep data exhibit a similar power law form:

$$\dot{\epsilon}^{ind} = \beta H^{(1/m)} \tag{9}$$

where $\dot{\epsilon}^{ind} = \frac{\dot{h}}{h}$ and $\beta$ is a constant that depends on material creep parameters. Note that the estimation of strain rate sensitivity through Eq. (9) does not require a $\beta$ to $\alpha$ conversion. It might explain why the accurate determination of the representative strain rate for power law creeping solids have been explored only by a few authors [8,20,36].

As demonstrated by Ginder et al. [20], the pioneering work of Bower et al. [6] leads to the following relation between $\alpha$ and $\beta$:

$$\alpha = \beta \frac{F^{(1/m)}}{c \tan\theta} \tag{10}$$

where $F$ and $c$ are functions of strain rate sensitivity $m$ and weakly dependent on $\theta$ [31]. These parameters are identified from finite element calculations [6]. Ginder et al. [20] proposed an extension of this work through the expanding cavity concept introduced by Johnson [33] that leads to an explicit expression for $F$. It leads to:

$$\alpha = \beta \frac{1}{c \tan\theta} \left( \frac{2}{3m} \right)^{(1/m)} \tag{11}$$

where $c$ remains a function of strain rate sensitivity $m$. These two papers pointed out that the conversion from $\alpha$ to $\beta$ can be written as:

$$\beta = \alpha \tan\theta f_1(m) \tag{12}$$

Reporting this expression in Eq. (9) and assuming that hardness $H$ is proportional to representative stress $\sigma_r$ through the constraint factor $H = \gamma\sigma_r$, it comes:

$$\dot{\epsilon}_r = f_2(m) \cot\theta \frac{\dot{h}}{h} = \alpha \sigma_r^{(1/m)} \tag{13}$$

This development clearly demonstrates that the representative strain rate in the framework of power law creeping solids is a function of strain rate sensitivity $m$.

In a complementary framework – indentation of glassy polymers (elastic-viscoplastic solids) – Kermouche et al. [8] and Rabemananjara et al. [37] came to a similar conclusion. Kermouche et al. [8,38] eventually evidenced from finite element simulations that $f_2$ can be expressed as:

$$f_2(m) = 0.44 \exp\left( \frac{0.2}{m} \right) \tag{14}$$

In the following, the relevance of this conversion (Eq. (13)) will be assessed by comparing the uniaxial compression creep behavior of amorphous selenium to the strain rate corrected indentation creep results.

It has been first required to fit the evolution of the indentation strain rate sensitivity $m$ with indentation strain rate to compute $f_2(m)$ as shown in Fig. 5. These power-law fits do not aim to represent the evolution of indentation strain rate sensitivity $m$ on a larger strain rate range than the experimental one.

The resulting representative strain rate $\dot{\epsilon}_r$ (Eq. (13)) for creep and CSR tests together with the relaxation strain rate $\dot{\epsilon}^{rel}$ (Eq. (3)) for relaxation tests are displayed as a function of representative stress $\sigma_r$ (Eq. (4)) in Fig. 6. A very good match between constant strain rate, indentation creep and indentation relaxation is observed. Macroscopic compression data from Su et al. [31] are also plotted on the same graph for temperatures of 30 °C and 36 °C. Here again, the agreement is very good, highlighting how this definition of the representative strain rate can be used to measure quantitative creep data from indentation creep.

Bower et al. [6] and Ginder et al. [20] also proposed a method to shift indentation data to match uniaxial creep data using $\beta$ to $\alpha$ conversion factors from Eq. (10) and (11). However, they use analytical solutions derived from contact mechanics and applied to power law creeping solids instead of the representative strain rate concept. Their methods are well suited for creep and CSR tests since the indentation strain rate is expressed as $\frac{\dot{h}}{h}$ but they would not be able to shift the indentation relaxation data, where strain rate is expressed from Eq. (3).

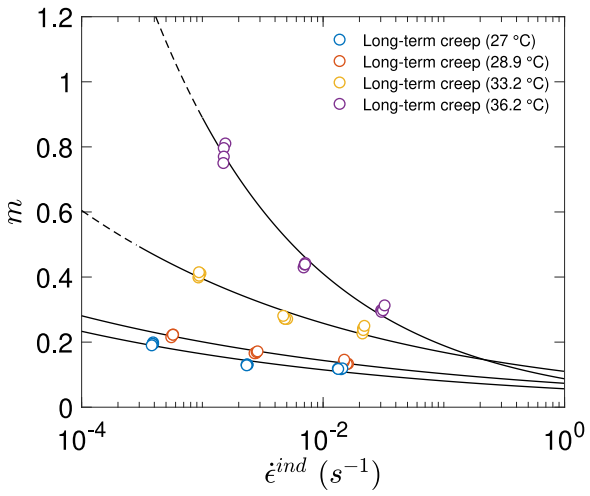


**Fig. 5.** Strain rate sensitivity $m$ as a function of indentation strain rate $\dot{\epsilon}^{ind}$ calculated from long-term creep tests at 27 °C, 30 °C, 33 °C and 36 °C. Plain lines represent the power-law functions fitted to the data. These fits do not aim to represent the evolution of indentation strain rate sensitivity $m$ on a larger strain rate range than the experimental one.

The authors emphasize that switching from indentation strain rate to representative strain rate with the proposed method is straightforward with indentation creep tests. The first step is to measure strain rate sensitivity $m$ as a function of indentation strain rate and then to compute the representative strain rate from Eq. (13). This is a fairly easy correction that can be used on any indentation creep data, as long as the strain rate sensitivity is higher than 0.1. This correction is needed when strain rate sensitivity is higher than 0.1 which does not occur in most of materials at room temperature. With increasing needs to measure viscoplastic properties at high temperature, the method proposed in this paper might be very useful since it can be applied to indentation creep standards.

It shall be noted that the results of this paper have been obtained on a material that is known to exhibit power law stationary creep near room temperature. When materials are known to exhibit also significant primary creep, it is well accepted that common indentation creep experiments can lead to unsatisfying results [15,39]. Indeed, the continuously increasing affected volume under constant load or constant contact pressure segment would lead to more and more materials entering primary creep. Indentation relaxation experiments, based on a nearly-constant affected volume, should be less affected by such issues. The good agreement between indentation creep and indentation relaxation data observed in this paper makes us confident to apply indentation relaxation in such context.

Moreover, indentation relaxation allows to attain very low strain rate within a relatively short time duration. Indeed, for the same hold time – 30 min for selenium, in this study – long-term indentation creep tests give access to $[10^{-5},\ 10^{-2}]$ $s^{-1}$ strain rate range and long-term relaxation tests $[10^{-6},\ 10^{-3}]$ $s^{-1}$. Indentation relaxation tests are therefore complementary to conventional indentation creep and CSR tests and make the measurement of strain rate sensitivity or activation energy possible within a broad strain rate range — i.e. $[10^{-6},\ 10^{0}]$ $s^{-1}$.

## 5. Conclusion

In this paper, indentation relaxation and indentation creep tests are compared on a model material which is amorphous selenium. The main conclusions are:

- A shift in the strain rate *vs.* hardness curves is observed between indentation creep and indentation relaxation results when strain rate sensitivity is higher than $m = 0.1$.

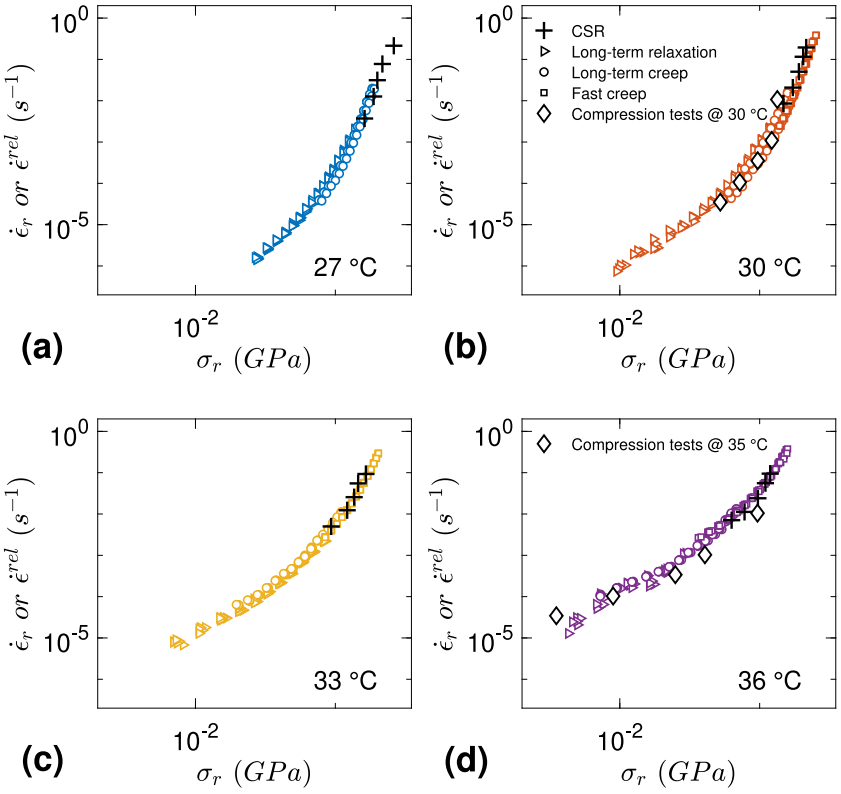


**Fig. 6.** Indentation creep behavior of amorphous selenium expressed with the representative strain rate $\dot{\epsilon}_r$ and stress $\sigma_r$ and measured from CSR (plus symbols), fast creep (square symbols), long-term creep (circle symbols) and relaxation (right pointing triangle symbols) at different temperatures: (a) 27 °C, (b) 30 °C, (c) 33 °C and (d) 36 °C. Diamond symbols are compression data from [31].

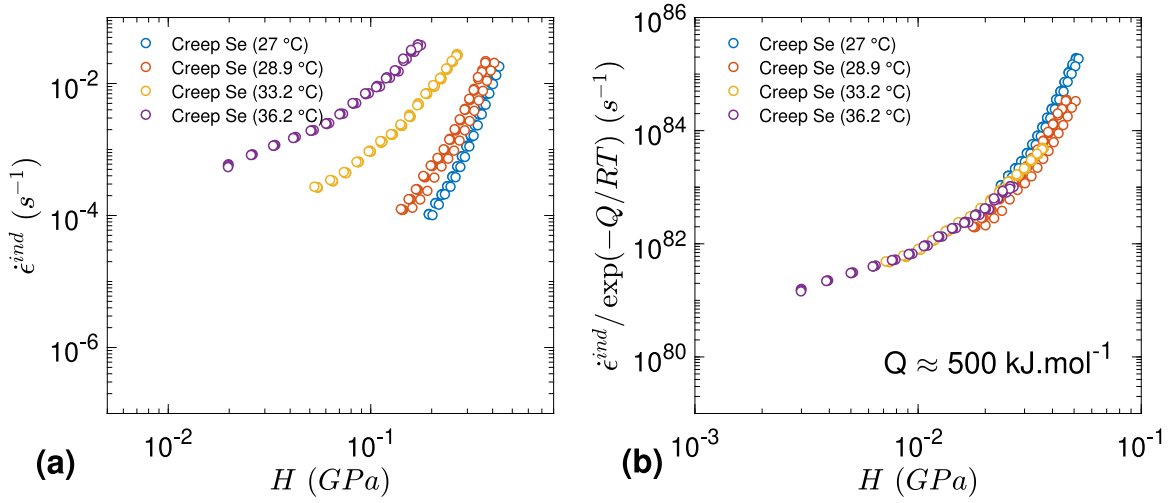


**Fig. 7.** Indentation creep behavior of amorphous selenium measured from creep tests at different temperatures (a) and temperature compensated indentation strain rate as a function of normalized hardness (b).

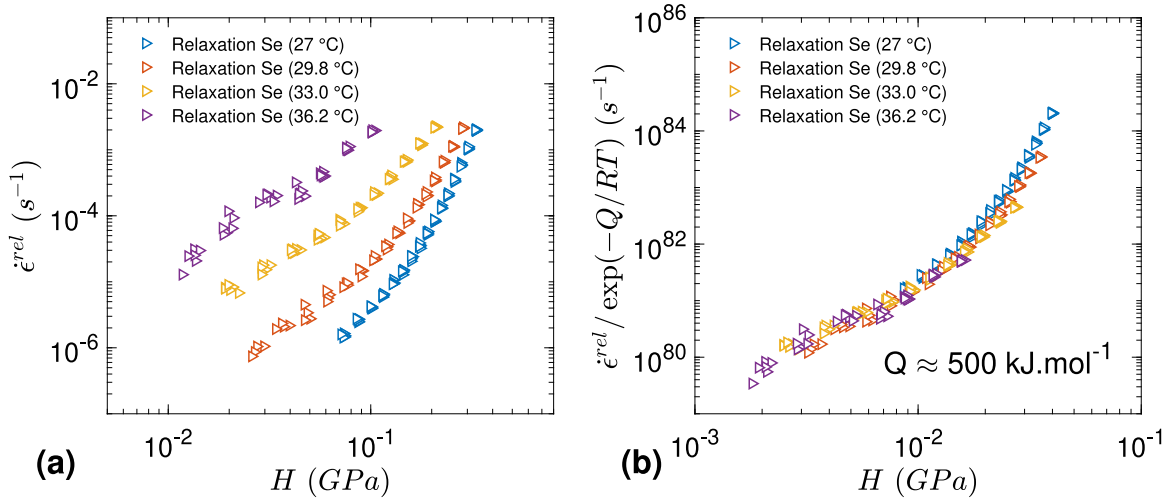


**Fig. 8.** Indentation creep behavior of amorphous selenium measured from relaxation tests at different temperatures (a) and temperature compensated representative strain rate as a function of normalized hardness (b).

- This shift is a matter of strain rate definition used to plot the curves.
- Several authors already pointed out that representative strain rate in indentation depends on strain rate sensitivity.
- The use of representative strain rate definition proposed by Kermouche et al. [8] leads to an almost perfect match between constant strain rate, indentation creep, indentation relaxation and macroscopic data for $m = 0.1$.

As a matter of fact, it is thus suggested to switch the definition of the strain rate from indentation strain rate (Eq. (9)) to representative strain rate (Eq. (15)), for materials with $m \geq 0.1$.

$$\dot{\epsilon}_r = 0.44 \exp\left(\frac{0.2}{m}\right) \cot\theta \frac{\dot{h}}{h} \tag{15}$$

## Data availability

The raw data required to reproduce these findings cannot be shared at this time due to time limitations. The processed data required to reproduce these findings cannot be shared at this time due to time limitations.

## CRediT authorship contribution statement

**Paul Baral:** Data curation, Writing - original draft. **Guillaume Kermouche:** Writing - original draft, Supervision. **Gaylord Guillonneau:** Funding acquisition, Writing - review & editing. **Gabrielle Tiphene:** Writing - review & editing. **Jean-Michel Bergheau:** Writing - review & editing. **Warren C. Oliver:** Conceptualization, Methodology, Software. **Jean-Luc Loubet:** Conceptualization, Project administration.

## Acknowledgments

This work was supported by the LABEX MANUTECH-SISE (ANR-10-LABX-0075) of Université de Lyon within the program "Investissements d'Avenir" (ANR-11-IDEX-0007) operated by the French National Agency (ANR). The authors thank also the financial support from Institut Carnot Ingénierie@Lyon, France and Institut Carnot M.I.N.E.S, France.

## Appendix

### *Apparent activation energy*

In this appendix it is proposed to compute apparent activation energy of amorphous selenium from indentation creep and relaxation. As this investigation is not central to the main message of this paper, it has thus been chosen not to include it in the core of the paper.

Estimation of activation energy $Q$ relies on the assumption that the indented material can be described using a Northon–Hoff law:

$$\dot{\epsilon} = \dot{\epsilon}_0 \sigma^{(1/m)} \exp\left(-\frac{Q}{RT}\right) \tag{16}$$

With $\dot{\epsilon}_0$ a constant, $m$ the strain rate sensitivity, $R$ the universal gas constant, $T$ the absolute temperature and $Q$ the activation energy. The apparent activation energy can thus be calculated from the slope of natural logarithm of strain rate *vs.* the inverse of the absolute temperature at a given stress $\sigma$. Here, $\dot{\epsilon}$ represents the uniaxial definition of strain rate. However, in the following developments $\dot{\epsilon}^{ind}$ and $\dot{\epsilon}^{rel}$ will be used instead to calculate the apparent activation energy from constant strain rate/creep and relaxation tests, respectively.

Figs. 7a and 8a display the creep behavior of amorphous selenium at different temperatures for long-term creep tests and long-term relaxation, respectively. The apparent activation energy for the amorphous selenium near its glass transition has been estimated from Eq. (16) by plotting the temperature compensated indentation strain rate $\dot{\epsilon}^{ind}/\exp(-Q/RT)$ as a function of the normalized hardness $H/E'$. Hence, an apparent activation energy of $Q \approx 500$ kJ mol$^{-1}$ leads to the best match for both creep (Fig. 8b) and relaxation (Fig. 4b). This result is in very good agreement with tensile relaxation tests performed by [40] (485 kJ mol$^{-1}$), the enthalpy relaxation experiments from [41] (448 kJ mol$^{-1}$) and indentation creep tests from [7] (495 kJ mol$^{-1}$), both at the glass transition. This means that both indentation creep and relaxation are well suited to measure the apparent activation energy $Q$.

It must be noticed that for fast creep and constant strain rate experiments, the apparent activation energies are significantly lower, with $Q \approx 420$ kJ mol$^{-1}$ and $Q \approx 320$ kJ mol$^{-1}$, respectively. Here, the stresses are high compared to common indentation creep and relaxation, and transients behavior may occur — i.e. power-law breakdown [31]. Norton–Hoff law applies to stationary creep and this assumption might be questionable for amorphous selenium over a large range of strain rate and temperature. Therefore, these points deserve to be investigated in a dedicated paper on the amorphous selenium creep behavior.

## References


[1] J.M. Wheeler, D.E.J. Armstrong, W. Heinz, R. Schwaiger, High temperature nanoindentation: The state of the art and future challenges, Curr. Opin. Solid State Mater. Sci. 19 (6) (2015) 354–366.

[2] P. Sudharshan Phani, W.C. Oliver, A direct comparison of high temperature nanoindentation creep and uniaxial creep measurements for commercial purity aluminum, Acta Mater. 111 (2016) 31–38.

[3] A.J. Harris, B.D. Beake, D.E.J. Armstrong, M.I. Davies, Development of high temperature nanoindentation methodology and its application in the nanoindentation of polycrystalline tungsten in vacuum to 950 °C, Exp. Mech. (2016) 1–12.

[4] B.D. Beake, A.J. Harris, J. Moghal, D.E.J. Armstrong, Temperature dependence of strain rate sensitivity, indentation size effects and pile-up in polycrystalline tungsten from 25 to 950 °C, Mater. Des. 156 (2018) 278–286.

[5] B.D. Beake, A.J. Harris, Nanomechanics to 1000 °C for high temperature mechanical properties of bulk materials and hard coatings, Vacuum 159 (October 2018) (2019) 17–28.

[6] A.F. Bower, N.A. Fleck, A. Needleman, N. Ogbonna, Indentation of a power law creeping solid, Proc. R. Soc. Lond. A 441 (1911) (1993) 97–124.

[7] W.H. Poisl, W.C. Oliver, B.D. Fabes, The relationship between indentation and uniaxial creep in amorphous selenium, J. Mater. Res. 10 (08) (1995) 2024–2032.

[8] G. Kermouche, J.L. Loubet, J.M. Bergheau, Extraction of stress–strain curves of elastic-viscoplastic solids using conical/pyramidal indentation testing with application to polymers, Mech. Mater. 40 (4–5) (2008) 271–283.

[9] B.N. Lucas, W.C. Oliver, G.M. Pharr, J.-L. Loubet, Time dependent deformation during indentation testing, MRS Proc. 436 (1) (1996) 233.

[10] D.S. Stone, J.E. Jakes, J. Puthoff, A.A. Elmustafa, Analysis of indentation creep, J. Mater. Res. 25 (4) (2010) 611–621.

[11] V. Maier, K. Durst, J. Mueller, B. Backes, H.W. Höppel, M. Göken, Nanoindentation strain-rate jump tests for determining the local strain-rate sensitivity in nanocrystalline Ni and ultrafine-grained Al, J. Mater. Res. 26 (11) (2011) 1421–1430.

[12] K. Durst, V. Maier, Dynamic nanoindentation testing for studying thermally activated processes from single to nanocrystalline metals, Curr. Opin. Solid State Mater. Sci. 19 (6) (2015) 340–353.

[13] P. Sudharshan Phani, W.C. Oliver, G.M. Pharr, On the measurement of power law creep parameters from instrumented indentation, JOM 69 (11) (2017) 2229–2236.

[14] O. Prach, C. Minnert, K.E. Johanns, K. Durst, A new nanoindentation creep technique using constant contact pressure, J. Mater. Res. 34 (14) (2019) 2492–2500.

[15] R. Goodall, T.W. Clyne, A critical appraisal of the extraction of creep parameters from nanoindentation data obtained at room temperature, Acta Mater. 54 (20) (2006) 5489–5499.

[16] P. Baral, G. Guillonneau, G. Kermouche, J.-M. Bergheau, J.-L. Loubet, Theoretical and experimental analysis of indentation relaxation test, J. Mater. Res. 32 (12) (2017) 2286–2296.

[17] P. Baral, G. Guillonneau, G. Kermouche, J.-M. Bergheau, J.-L. Loubet, A new long-term indentation relaxation method to measure creep properties at the micro-scale with application to fused silica and PMMA, Mech. Mater. 137 (2019) 103095.

[18] S.a. Syed Asif, J.B. Pethica, Nanoindentation creep of single-crystal tungsten and gallium arsenide, Phil. Mag. A 76 (6) (1997) 1105–1118.

[19] V. Maier, B. Merle, M. Göken, K. Durst, An improved long-term nanoindentation creep testing approach for studying the local deformation processes in nanocrystalline metals at room and elevated temperatures, J. Mater. Res. 28 (09) (2013) 1177–1188.

[20] R.S. Ginder, W.D. Nix, G.M. Pharr, A simple model for indentation creep, J. Mech. Phys. Solids 112 (2018) 552–562.

[21] M. Sakai, M. Sasaki, A. Matsuda, Indentation stress relaxation of sol–gel-derived organic/inorganic hybrid coating, Acta Mater. 53 (16) (2005) 4455–4462.

[22] C.Y. Zhang, Y.W. Zhang, K.Y. Zeng, L. Shen, Y.Y. Wang, Extracting the elastic and viscoelastic properties of a polymeric film using a sharp indentation relaxation test, J. Mater. Res. 21 (12) (2006) 2991–3000.

[23] G. Kermouche, J.L. Loubet, J.M. Bergheau, An approximate solution to the problem of cone or wedge indentation of elastoplastic solids, C. R. Mec. 333 (5) (2005) 389–395.

[24] A.A. Elmustafa, S. Kose, D.S. Stone, The strain-rate sensitivity of the hardness in indentation creep, J. Mater. Res. 22 (04) (2007) 926–936.

[25] G. Kermouche, J.L. Loubet, J.M. Bergheau, A new index to estimate the strain rate sensitivity of glassy polymers using conical/pyramidal indentation, Phil. Mag. 86 (33–35) (2006) 5667–5677.

[26] J.B. Pethica, W.C. Oliver, Tip surface interactions in STM and AFM, Phys. Scr. T19A (1987) 61–66.

[27] W.C. Oliver, G.M. Pharr, An improved technique for determining hardness and elastic modulus using load and displacement sensing indentation experiments, J. Mater. Res. 07 (06) (1992) 1564–1583.

[28] I.N. Sneddon, Boussinesq's problem for a rigid cone, Math. Proc. Camb. Phil. Soc. 44 (04) (1948) 492–507.

[29] J.L. Loubet, M. Bauer, A. Tonck, S. Bec, B. Gauthier-Manuel, Nanoindentation with a surface force apparatus, in: Mechanical Properties and Deformation Behavior of Materials Having Ultra-Fine Microstructures, Vol. 233, Springer Netherlands, Dordrecht, 1993, pp. 429–447.

[30] B. Merle, V. Maier-Kiener, G.M. Pharr, Influence of modulus-to-hardness ratio and harmonic parameters on continuous stiffness measurement during nanoindentation, Acta Mater. 134 (2017) 167–176.

[31] C. Su, E.G. Herbert, S. Sohn, J.A. LaManna, W.C. Oliver, George M. Pharr, Measurement of power-law creep parameters by instrumented indentation methods, J. Mech. Phys. Solids 61 (2) (2013) 517–536.

[32] D. Tabor, The hardness of solids, Rev. Phys. Technol. 1 (3) (1970) 145.

[33] K.L. Johnson, The correlation of indentation experiments, J. Mech. Phys. Solids 18 (2) (1970) 115–126.

[34] M. Dao, N. Chollacoop, K.J. Van Vliet, T.A. Venkatesh, S. Suresh, Computational modeling of the forward and reverse problems in instrumented sharp indentation, Acta Mater. 49 (19) (2001) 3899–3918.

[35] J.L. Bucaille, E. Felder, G. Hochstetter, Identification of the viscoplastic behavior of a polycarbonate based on experiments and numerical modeling of the nano-indentation test, J. Mater. Sci. 37 (18) (2002) 3999–4011.

[36] Y.T. Cheng, C.M. Cheng, Scaling, dimensional analysis and indentation measurements, Mater. Sci. Eng. R 44 (4–5) (2004) 91–150.

[37] L. Rabemananjara, X. Hernot, G. Mauvoisin, A. Gavrus, J.M. Collin, Formulation of a representative plastic strain and representative plastic strain rate by using a conical indentation on a rigid visco-plastic material, Mater. Des. 68 (October) (2015) 207–214.

[38] G. Kermouche, J.L. Loubet, J.M. Bergheau, Cone indentation of time-dependent materials: The effects of the indentation strain rate, Mech. Mater. 39 (1) (2007) 24–38.

[39] J. Dean, A. Bradbury, G. Aldrich-Smith, T.W. Clyne, A procedure for extracting primary and secondary creep parameters from nanoindentation data, Mech. Mater. 65 (2013) 124–134.

[40] R. Böhmer, C.A. Angell, Elastic and viscoelastic properties of amorphous selenium and identification of the phase transition between ring and chain structures, Phys. Rev. B 48 (9) (1993) 5857–5864.

[41] I. Echeverrìa, P.L. Kolek, D.J. Plazek, S.L. Simon, Enthalpy recovery, creep and creep–recovery measurements during physical aging of amorphous selenium, J. Non-Cryst. Solids 324 (3) (2003) 242–255.